POLDER-3 / PARASOL

Land Surface Algorithms Description

Issue 3.11

Prepared by Roselyne Lacaze (MEDIAS-France)
in collaboration with Fabienne Maignan (LSCE)

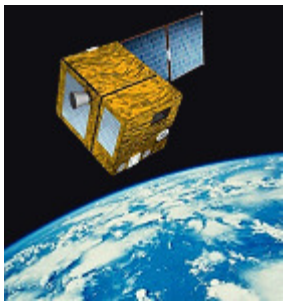

Issue 3.11 – July 28th 2010

Change Record

Issue/Rev	Date	Pages	Description of Change	Release
I1.00	06.03.2006	All		
I2.00	26.06.2006	16 to 21	Update of the parameters provided to users	
I3.00	10.04.2007	12 to 21	Update of the parameters provided to users after validation exercise: remove of vegetation variables, change of definition of DHR, change of coefficients for assessing broadband albedos.	
I3.10	13.06.2007	7 to 11	Update of the Level 2 algorithms description	
I3.11	28.07.2010	22	Change in the contact address	

Acronyms

ADEOS :	Advanced Earth Observing Satellite
BBHR :	Broadband Bi-hemispherical Reflectance
BDHR :	Broadband Directional Hemispheric Reflectance
BHR :	Bi-Hemispherical Reflectance
BPDF :	Bi-directional Polarized reflectance Distribution Function
BRDF :	Bi-directional Reflectance Distribution Function
CCD :	Charge Coupled Device
CNRM :	Centre National de Recherches Météorologiques
DHR :	Directional Hemispheric Reflectance
ECMWF :	European Center of Medium range Weather Forecast
GOME :	Global Ozone Monitoring Experiment
IGBP :	International Geosphere-Biosphere Program
LSCE :	Laboratoire des Sciences du Climat et de l'Environnement
NDVI :	Normalized Difference Vegetation Index
PARASOL :	Polarisation et Anisotropie des Réflectances au sommet de l'Atmosphère, couplées avec un Satellite d'Observation emportant un Lidar
POLDER :	POLarization and Directionality of Earth's Reflectances
SAGE :	Stratospheric Aerosol and Gas Experiment
TOA :	Top Of the Atmosphere
TOMS :	Total Ozone Mapping Sensor

Table of Content

List of figures

List of Tables

1. Introduction

Monitoring of terrestrial vegetation from satellites at global and regional scales requires accurate and frequent measurements of surface reflectance. In this context, the POLDER instrument leads a key improvement providing, at high temporal resolution, measurements of the Bi-directional Reflectance Distribution Function (BRDF) corrected for atmospheric effects.

The first algorithms of the "Land Surface" processing line have been applied to the 8 months of ADEOS-1/POLDER-1 data. The methodology, which takes advantage of the POLDER directionality, was presented in Leroy et al. (1997). Advanced algorithms have been developed to be applied to ADEOS-2/POLDER-2 data and to re-process ADEOS-1/POLDER-1 measurements. These algorithms are now applied to POLDER-3/PARASOL observations to get some preliminary products.

The POLDER-3 sensor on the PARASOL micro-satellite is similar to that of POLDER-1 & 2. It was launched in December 2004 to be part of the A-Train, flying in formation with AQUA, CALIPSO and CLOUDSAT. Significant changes concern:

- The orientation of the CCD matrix: on POLDER-1 & 2, the long axis of the matrix was cross-track; on POLDER-3/PARASOL, it is along track. This results in a lower daily coverage of the Earth, but a larger directional sampling for the pixels that are in the instrument swath (up to 16 from 14 on POLDER-1 & 2)
- The shorter wavelength polarized channel is at 490 nm instead of 443 nm on POLDER-1 & 2.
- On POLDER-1 & 2 there were two channels at 443 nm (for optimised dynamic and signal to noise). There is a single one on POLDER-3, but with an additional channel at 1020 nm. This channel may be used for optimised synergy with the CALIPSO measurements at 1060 nm.

2. Land Surface Level 2 Algorithms

The "Land Surface" Level 2 processing line generates the bi-directional surface reflectances from the Top of the Atmosphere observations. First, the cloudy pixels are removed, and then, the measurements are corrected from the effects of absorbing gazes and aerosols (Figure 1).

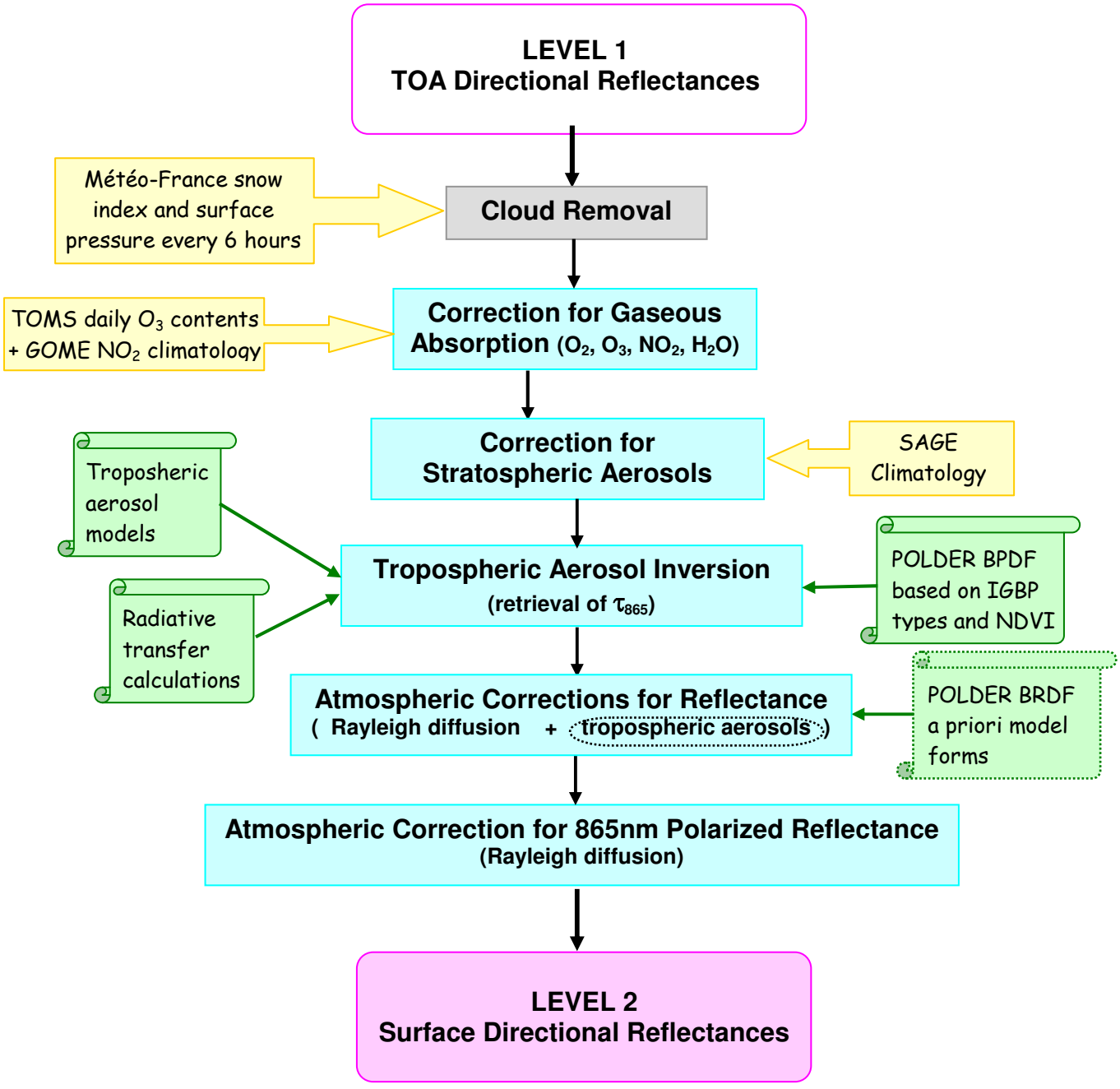

Figure 1 : Land Surface Level 2 processing scheme

(yellow: exogen data; green: look-up tables)

2.1. The cloud detection

The cloud filtering takes advantage of the POLDER multi-spectral and multi-directional specific characteristics. Four tests are applied to every POLDER pixel at the full resolution. These tests are non-exclusive and one proved positive is sufficient to declare the pixel cloudy. They consist in:

1. comparing the apparent pressure in oxygen band to the surface pressure
2. comparing the reflectance in the blue channel with a threshold
3. considering the directional variability of the surface reflectance to eliminate the partial cloud covers
4. detecting the presence of polarized rainbow, indicative of the presence of water droplets.

Once all these tests are applied, some of the pixels declared cloudy by the blue channel test are considered again in order to prevent from abusive elimination of actually clear pixels. It is highly probable to be the case above snow covers. This kind of difficulty is also encountered with the apparent pressure test above dense forests.

Finally, pixels adjacent to two detected clouds are considered to be contaminated and are rejected for further processing.

Performances of this cloud detection scheme have been evaluated against ground-based sky observations. More details about this validation or about the detection method itself can be found in Bréon and Colzy (1999).

2.1.1. Test 1: apparent pressure in O_2 band

It involves two POLDER channels of different width (a narrow one of 10 nm and a broader one of 40 nm) centered on the oxygen "A" absorption band at 765 nm. The ratio of the reflectances measured in each of these two channels is a good indicator of the atmospheric oxygen absorption (Bréon and Bouffiès, 1996). From this ratio, an apparent pressure of the reflector can be derived that is a physical quantity directly comparable to surface pressure. A large difference is indicative of the presence of a cloud layer since these scattering layers (in particular high clouds) have a large effect on the apparent pressure (Bréon and Clozy, 1999). The pixel is declared cloudy if $(P_{surf} – P_{app}) > \Delta P$, where P_{app} results from the average over all available viewing angles in order to reduce random uncertainties. A clear surface shows a spectral signature that affects the apparent pressure (lower apparent pressure over the vegetation). Consequently, the threshold depends on the vegetation coverage, quantified by the NDVI. Bréon and Bouffiès (1996) highlighted that the difference $(P_{surf} - P_{app})$ is NDVI-dependant. An empirical representation of $(P_{surf} - P_{app}) = f(NDVI)$ for clear sky cases enabled to advance a linear relation $\Delta P = a * NDVI + b$ with a=50 and b=210. The NDVI is the average value over the different viewing directions. The surface pressure in an output of the ECMWF meteorological forecast model.

2.1.2. Test 2: threshold on blue channel reflectance

While ground reflectance increases with wavelength in visible and near-infrared, cloud reflectance is roughly uniform over this spectral range. Thus, the contrast between ground and cloud reflectances is the largest in the blue channel. However, this test cannot be applied to raw blue measurements as long as the molecular diffusion dominates the signal and screens the ground signature. Also, this test declares a pixel cloudy if R_{490nm} corrected from molecular diffusion is above a given threshold, Δ_{443}: ($R_{490} - R_{490mol} > \Delta_{443}$). The Δ_{443} threshold takes into account the spatial variability of the surface reflectance. For that, a base of surface reflectances R_{443min} has been constructed using the Directional Hemispheric Reflectances (DHR) calculated from the 8 months of POLDER-1 data. The pixel is declared cloudy when ($R_{490} - R_{490mol}$) > ($R_{443min} + \Delta'$) where Δ' is fixed to 0.1, assuming that the reflectance increase due to vegetation growth during the annual cycle does not exceed this rate.

2.1.3. Test 3: directional variability

This test is specific to POLDER, thanks to the multi-directional measurements. The TOA reflectance is rather isotropic in presence of a continuous cloud cover, but it is no more the case with broken cloudiness. Such a mixed meteorological situation, when occurring at POLDER pixel scale, is difficult to capture with the other three cloud tests. Adding in the cloud detection algorithm a criteria based on directional variability of Earth reflectance (in the blue channel) provides a good tool for recognition of these sub-pixel cloud cover.

Variability of directional reflectance measurements is estimated through the RMS of the distance to a polynomial fit established over all viewing geometry configurations (hereafter referred as RMSdir). The criteria applied to statute whether the considered pixel contains or not partial clouds is a simple threshold. This threshold has been empirically determined by comparison of the calculated POLDER directional variability and meteorological measurements in points of synoptic stations. If the RMSdir overcomes the given threshold, the pixel is classified as cloudy.

2.1.4. Test 4: polarized rainbow

In presence of liquid water clouds, the reflected radiance shows a maximum in the 142° scattering direction and this maximum is highly polarized. This property is exploited through multi-directional and polarized POLDER data. The test on the presence of a polarized rainbow is realized in the 865 nm channel, the less contaminated by atmosphere (molecules and aerosols) single scattering. If R_{865pol} within 142° is significantly larger than R_{865pol} away from this direction, the pixel is declared cloudy.

2.1.5. Case of snow cover

Since snow has a large radiance in the blue channel, and shows a spectral signature very similar to that of the clouds (in the spectral range covered by POLDER), the test of the threshold on the blue channel fails, declaring snow pixels as cloudy. Although it appears not possible to unambiguously distinguish thin clouds from partial snow, it is useful to distinguish at least thick clouds from uniform snow covered region.

In configuration of

- negative P_{app} test
- negative polarized rainbow test

- positive R_{490} test
- large reflectance at 670nm
- pixel identified snow or ice by meteorological data,

the pixel is put back to clear.

2.1.6. Case of dense forests

Tropical forests show a specific spectral signature. The surface reflectance, averaged over the narrow "763nm" channel is significantly larger than that on the wide "765nm" channel, when the apparent surface pressure algorithm assumes a spectrally neutral surface. This signature yields false cloud detection. To correct this problem, the pixels that are declared cloudy by the Apparent Pressure test are reconsidered.

In configuration of

- positive P_{app} test
- negative polarized rainbow test
- negative R_{490} test
- large NDVI,

the pixel is put back to clear.

2.2. The atmospheric correction

After cloudy pixels are removed, the TOA reflectances are corrected from the effects of absorbing gazes, stratospheric and troposheric aerosols.

2.2.1. Correction from gas absorption

The TOA radiances are divided by an a-priori ozone transmission, based on radiative transfer simulation driven by daily TOMS ozone retrievals.

The absorption of Nitrous Oxide (NO_2), which affects the blue channel of POLDER, is corrected using a monthly climatology based on GOME retrievals.

The water vapor absorption, which has a slight impact in near infrared channels mainly, is corrected using an empirical formula. This relationship between the sun-target-satellite geometry and the ratio of the 910 nm and 865 nm measurements is based upon radiative simulations. As the 910 nm channel is centered on a water vapor absorption band, the ratio of 910 nm and 865 nm data is mostly a function of water vapor content.

The 763 nm and 765 nm channels are both centered on the oxygen A absorption band. The 763 nm channel is much more affected because it is four times narrower. An empirical formula based on the two channels measurements yields an oxygen "absorption free" estimate of the radiance.

2.2.2. Stratospheric aerosol scattering correction

The stratospheric aerosols are generated mostly by large volcanic eruptions. The corresponding optical thickness is, a few months after the eruption, well mixed over

latitudinal bands. Ground based as well as satellite limb measurements yield a stratospheric aerosol optical thickness. POLDER land surface algorithm is designed to make use of such estimated for a correction of the stratospheric aerosol scattering. The correction is based on an a-priori stratospheric aerosol model.

2.2.3. Atmospheric scattering correction

The TOA reflectances are simultaneously corrected from Rayleigh scattering and partly from the scattering and absorption due to tropospheric aerosols, taking into account for the surface BRDF. It consists in inverting the radiative transfer equation (Eq.1):

Eq. 1
$$\rho_{TOA} = A(\theta_S,\theta_V,\phi,z,\tau,imod,iBRDF)\ \rho_S^2 + B(\theta_S,\theta_V,\phi,z,\tau,imod,iBRDF)\ \rho_S + C(\theta_S,\theta_V,\phi,z,\tau,imod,iBRDF)$$

where θ_S, θ_V, ϕ are the sun zenith, the view zenith, and the relative azimuth angles, z is the altitude, τ is the optical thickness at 865 nm, imod is the aerosol model, and iBRDF represents an a-priori BRDF model.

Whereas the preceding version of this algorithm used only a fixed aerosol model and the corresponding inverted optical thickness, we now consider that the outputs of the aerosol inversion algorithm are sufficiently reliable to use them for our atmospheric correction.

Because the radiative transfer computations are too much time consuming to be included in the processing line, values of coefficients A, B, C of Eq. 1 are calculated using the radiative transfer code 6S (Vermote et al., 1997) and stored in look-up-tables for each of the five wavebands.

On the other hand, the coefficients of Roujean model (Roujean et al., 1992) inverted against the 8 months of POLDER-1 measurements have been analysed to identify 3 great BRDF types: one quasi-isotropic standing for desert and snow, one for developed forest, and one last for intermediate vegetations.

The algorithm relies on 4 steps:

- selection of BRDF form: a first inversion of the surface reflectance is done at 865 nm using the Lambertian hypothesis. In this case, the surface reflectance is linearly related to the TOA reflectance. This inversion provides a BRDF section. The predefined BRDF which gives the nearest form for the same section (using a least-squares criterion) is selected.
- The aerosol inversion algorithm identifies the “best” aerosol model among a set of 10 and calculates the corresponding optical thickness at 865 nm.
- A multi-linear interpolation of coefficients A, B, C is performed for dimensions other than imod and iBRDF.
- Then, the positive root of Eq. 1 finally gives the surface reflectance ρ_S (Eq. 2):

Eq. 2

$$\rho_S = \frac{-B + \sqrt{B^2 - 4 * A * (C - \rho_{TOA})}}{2 * A}$$

3. Land Surface Level 3 algorithms

The Land Surface Level 3 processing line generates (Figure 2):

- The 3 directional coefficients, and their errors, resulting from the inversion of a BRDF model (Maignan et al., 2004).
- The spectral Directional-Hemispherical Reflectances (DHR), the spectral Bi-hemispherical Reflectances (BHR), the broadband DHR and BHR in the visible [400nm, 700nm], and over the whole spectrum [300, 4000nm], and the Normalized Difference Vegetation Index (NDVI) corrected for directional effects. An error is associated to each variable.

The “Land Surface” Level 3 algorithm relies on 3 major steps (Figure 2):

- the filtering module
- the linear inversion of a BRDF model

3.1. The filtering module

The multi-directional spectral reflectances are the inputs of the “Land Surface” Level 3 processing line. Their quality controls the relevance of biophysical parameters. In order to eliminate contaminated measurements not detected by the Level 2 cloud detection and atmospheric corrections, a multi-temporal filtering module has been developed.

The filtering module is applied to 490 nm bi-directional reflectances. Indeed, in this spectral range, the land surface reflectance is low and the measured signal is largely due to atmospheric interactions such as gaseous absorption, Rayleigh scattering and aerosol effects. In order to reduce the impact of the bi-directional effects, the analysis is performed on the measurements acquired in the perpendicular plane. All POLDER wavebands are affected by the results of the filtering.

The filtering module is applied under the assumption that disturbed acquisitions are few regarding to the whole BRDF measurements, and that the selected acquisition in the track is representative of the whole track. For a given pixel, a track consists of a maximum of 14 observations acquired during an overpass. Moreover, it assumes that the land surface properties are stable during the synthesis period. Then, the main temporal inconsistencies of measurements are due to cloud and/or aerosols.

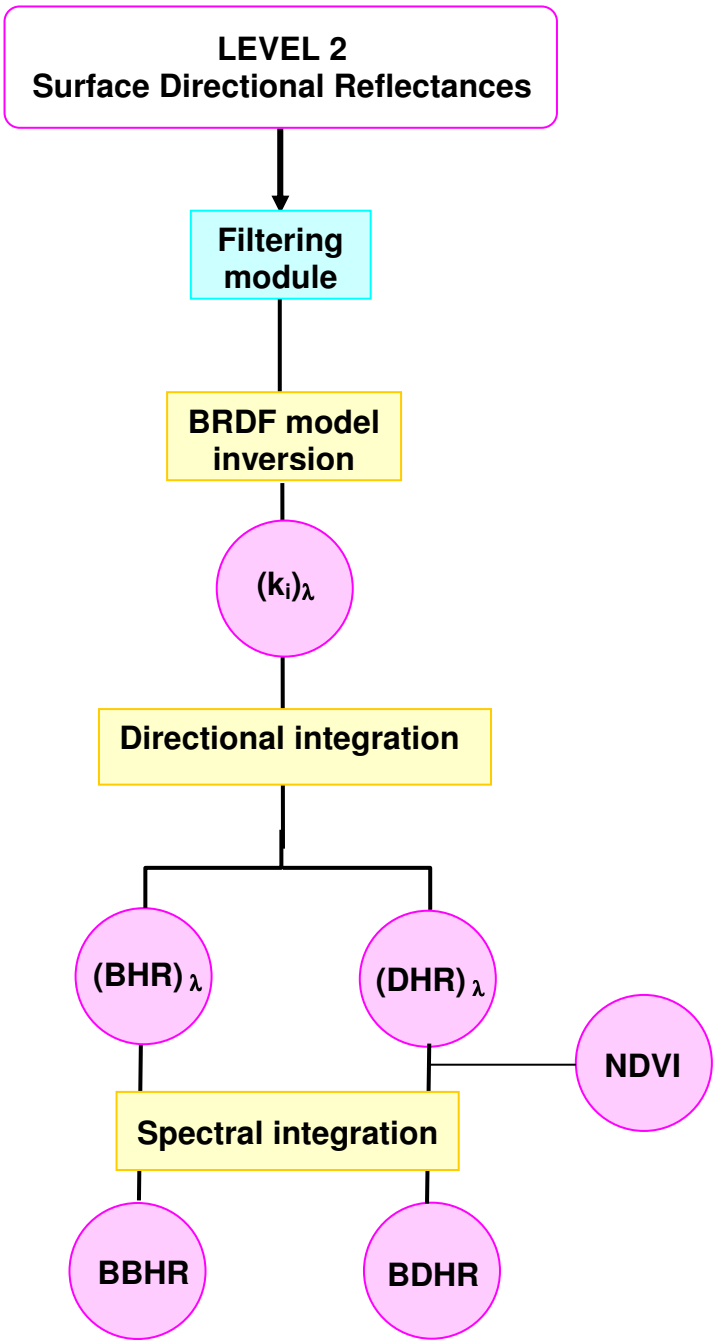

Figure 2 : Outline of the Level 3 Land Surface processing line

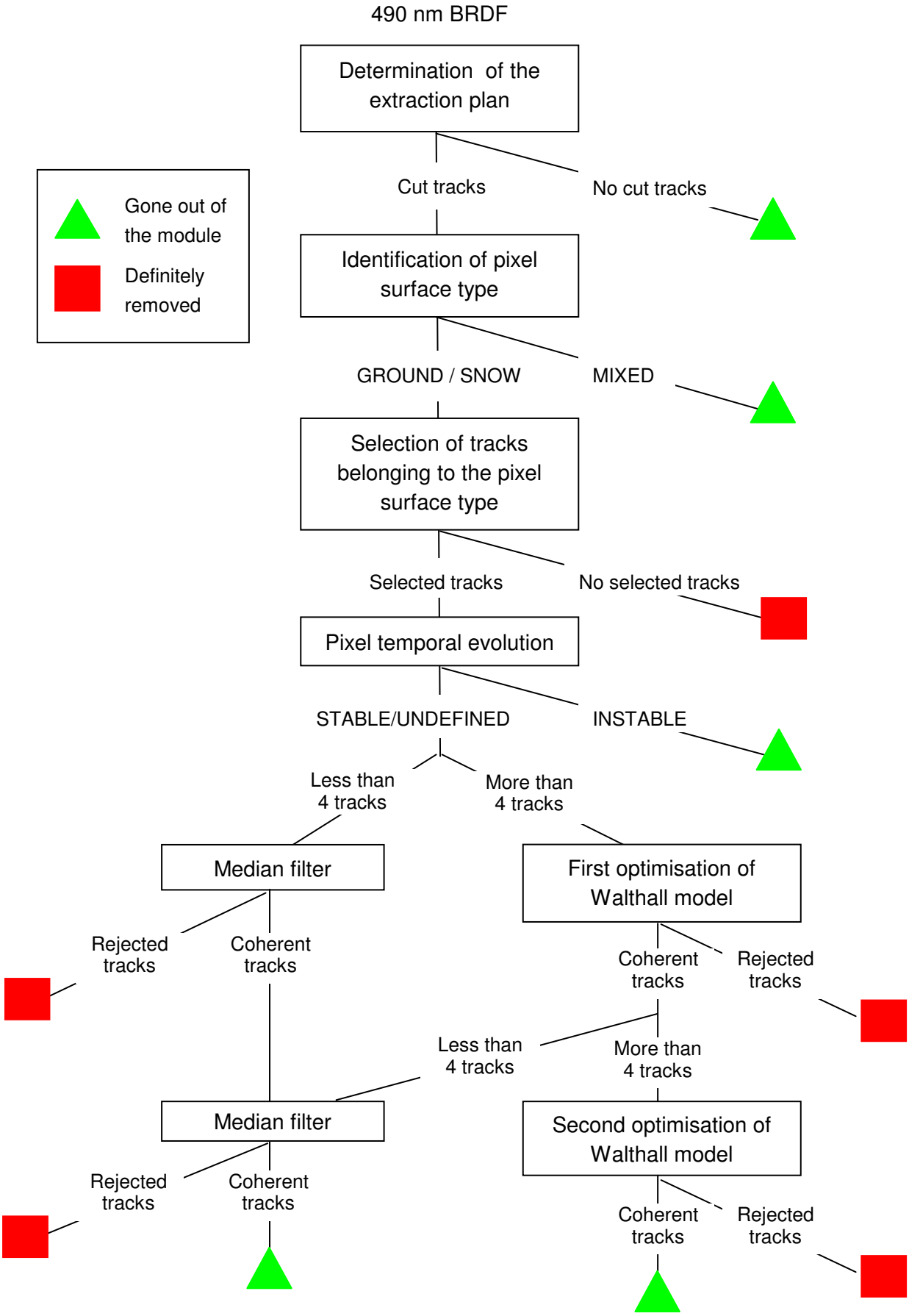

Figure 3 : Functional scheme of the temporal filtering module

The filtering module relies on 3 steps according the functional scheme in Figure 3:

1. Selection of the acquisition closest to the perpendicular plane for each POLDER track during the synthesis period.
2. Determination of surface type (ground, snow or mixed) and of its temporal evolution over the synthesis period.
3. Fitting the directional model of Walthall (1985) to remove the noisy measurements.

The first step consists in extracting one representative measurement per track. For that, the algorithm identifies the tracks direction by analysing the viewing azimuth angle evolution on successive observations, which determines the extraction plane: the closest plane to the perpendicular plane that cuts the greatest number of tracks. The no-cut tracks go out of the filtering module. Then, the measurement of each cut track which minimises the angular distance with the extraction plan is selected.

The determination of the surface type is performed using acquisitions during the central 10-day period. Each acquisition is associated with one of the three classes (SNOW, MIXED, GROUND) defined according to the following thresholds:

- SNOW for 490 nm reflectance greater than 0.3
- MIXED for 490 nm reflectance between 0.2 and 0.3
- GROUND for 490 nm reflectance lower than 0.2

The pixel is associated with the majority class. Tracks belonging to the minority classes are definitely removed. If the cardinals of two classes are equal, the pixel is considered as MIXED. The MIXED pixels go out of the filtering module. The temporal evolution of SNOW and GROUND pixels is analysed. If the number of remaining measurements is greater than 6 and are distributed, at least, over a week, a linear relationship is fitted by a least mean square minimisation. For other cases, the temporal evolution of the pixel is UNDEFINED. If the retrieved slope is between –0.05 and 0.05 (R/orbit), the pixel is considered as STABLE over the synthesis period, else it is considered as INSTABLE. The INSTABLE pixels go out of the filtering module.

The third step is applied to SNOW and GROUND pixels whose temporal evolution is STABLE or UNDEFINED. If there are more than 4 remaining measurements, a linear empirical reflectance model (Walthall, 1985) is fitted using a least mean square minimisation procedure. The acquisitions for which the difference between modelled and measured reflectances are larger than 0.025 for a GROUND pixel (0.1 for a SNOW pixel) are definitely removed from for the processing. If the remaining measurements are not numerous enough to invert the Walthall model, the acquisitions that deviate more than 0.1 from the median reflectance value are considered as noisy and removed. This alternative option is less relevant but can be applied in any cases, especially when a small number of clear tracks are available as in equatorial areas, where it allows to eliminate some residual cloud contamination. A second adjustment is performed under the same conditions of number of remaining measurements than the first one.

3.2. The BRDF model inversion and the semi-empirical approach

A new linear semi-empirical BRDF model proposed by Maignan et al. (2004) has been implemented in the Level 3 processing line to normalize bi-directional POLDER measurements. It follows the general formulation (Eq. 3) of the bi-directional reflectance $R(\theta_s, \theta_v, \varphi)$ defined by Roujean et al. (1992):

Eq. 3
$$R(\theta_s,\theta_v,\varphi) = k_0 + k_1 * F_1(\theta_s,\theta_v,\varphi) + k_2 * F_2(\theta_s,\theta_v,\varphi)$$

where θ_s, θ_v and φ are the solar zenith, view zenith and relative azimuth angles respectively, F_i are a-priori kernels based on either physical or empirical considerations, and k_i are free parameters to be inverted on the measurements.

This model combines the reciprocal geometric kernel of "Li_sparse" (Lucht et al., 2000) (Eq. 4) with the volumic kernel of "Ross_thick" (Roujean et al., 1992) merged with a hotspot module (Bréon et al., 2002). The modified version of volumic kernel (Eq. 5) allows to reproduce accurately the hotspot phenomenon.

Eq. 4
$$F_1 = \frac{m}{\pi}(t - \sin t \cos t - 1) + \frac{1+\cos\xi}{2\cos\theta_s \cos\theta_v}$$
$$\cos t = \frac{2}{m}\sqrt{\Delta^2 + (\tan\theta_s \tan\theta_v \sin\varphi)^2}$$
$$m = \frac{1}{\cos\theta_s} + \frac{1}{\cos\theta_v}$$

Eq. 5
$$F_2(\theta_s,\theta_v,\varphi) = \frac{4}{3\pi}\frac{1}{\cos\theta_s + \cos\theta_v}\left[\left(\frac{\pi}{2} - \xi\right)\cos\xi + \sin\xi\right]\left(1 + \left(1 + \frac{\xi}{\xi_0}\right)^{-1}\right) - \frac{1}{3}$$

where ξ is the phase angle given by $\cos\xi = \cos\theta_s \cos\theta_v + \sin\theta_s \sin\theta_v \cos\varphi$, and ξ_0 is a characteristic angle that can be related to the ratio of scattering element size and the canopy vertical density. ξ_0 is set to 1.5° to avoid the addition of a free parameter in the BRDF modelling. Δ is related to the horizontal distance between the projections of sun and viewing directions:

$$\Delta(\theta_s,\theta_v,\varphi) = \sqrt{\tan^2\theta_s + \tan^2\theta_v - 2\tan\theta_s \tan\theta_v \cos\varphi}$$

A temporal weighting gives more weights to the acquisitions close in time to the centre of the synthesis period. The weighting function is a gaussian curve based on the central track of the synthesis period (Eq. 6). Its standard deviation is equal to half the number of tracks during the synthesis period. The temporal weighting enhances the seasonal variations of hemispherical reflectances and NDVI, then the changes of surface properties are more accurately represented.

Eq. 6

$$W_i = \exp\left(-\frac{1}{2}\left(\frac{t_i - t_c}{hw} \right)^2 \right)$$

W_i is the weight applied to the track i of track number t_i, t_c is the track number of the central track of the synthesis period. hw is half the number of tracks during the synthesis period.

The model parameters [K] are inverted so as to minimize the root mean square difference between the measurements and the model values. For linear models, this inversion is a simple matrix inversion:

Eq. 7

$$[K] = ([F]^t [F])^{-1} [F]^t [R]$$

where [R] is a *1*x*N* matrix, representing the column vector of the *N* measured weighted reflectances and [F] is a *3*x*N* matrix, representing for each of the *3* kernels the column vector of the weighted kernel values for each of the *N* measurements geometries.

The inversion is carried out in 5 wavebands (490nm, 565nm, 670nm, 765nm, and 865nm). The resulting spectral directional coefficients [K] are:

- a nadir-zenith reflectance, k_0
- a roughness indicator, k_1
- a volume scattering indicator, k_2.

However, because of the correlation between the F_1 et F_2 kernels, the use of the directional coefficients taken independently as surface indicators should be cautious. Their optimal use is as a set of coefficients to accurately simulate the BRDF.

The error associated to each directional coefficients is estimated by the root mean square error (rmse) of the k_i distribution. It is represented by the root square of the diagonal elements of the variance-covariance matrix calculated during the BRDF model inversion. This method is not completely realistic because the directional kernels are not totally independent.

3.2.1. The spectral directional and hemispheric albedos

The directional coefficients resulting from the BRDF model inversion are used for computing the spectral Directional Hemispherical Reflectances (DHR), also called directional albedo or black-sky albedo, for the noon sun angle θ_{s_noon} of the reference date of the synthesis period (Eq. 8) as specified by CNRM/Météo-France.

Eq. 8

$$DHR(\theta_{s\_noon}) = k_0 + k_1 * G_1(\theta_{s\_noon}) + k_2 * G_2(\theta_{s\_noon})$$

where $G_i(\theta_s) = \frac{1}{\pi}\int_\Omega F_i(\theta_s, \theta_v, \varphi)\cos\theta_v d\omega$ is the integration of kernels F_i over the full viewing hemisphere. The integrals are approximated by pre-computed polynomial relationships of θ_s.

The associated error on spectral DHR are estimated by Eq. 9 where [COV] is the variance-covariance matrix of the linear regression.

Eq. 9 $$ErrDHR = \sqrt{[G]^t [COV][G]}$$

with

Eq. 10 $$[COV] = \sigma([F]^t[F]^{-1}) \quad \textbf{with} \quad \sigma = \frac{\|R\|^2 - [K]^t[F]^t[R]}{N-3}$$

The Directional coefficients resulting from the BRDF model inversion are also used for computing the spectral Bi-Hemispherical Reflectances (BHR), also called hemispheric albedo or white-sky albedo, for a sun angle integrated over the whole diurnal cycle (Eq. 11).

Eq. 11 $$BHR = k_0 + k_1 * H_1 + k_2 * H_2$$

where $H_i = \frac{1}{\pi}\int_{\theta s}\int_{\Omega} F_i(\theta_s, \theta_v, \varphi)\cos\theta_s \cos\theta_v \, d\omega \, d\theta_s$ is the integration of kernels F_i over the full viewing and illumination hemispheres.

The associated error on spectral BHR are estimated by Eq.12:

Eq. 12 $$ErrBHR = \sqrt{[H]^t[COV][H]}$$

The pre-computed polynomial relationships of θ_s, and the values of H_i have been specified by LSCE.

3.2.2. The broadband albedos

The spectral DHR and BHR are spectrally integrated over 2 broad bands:

- visible [400 – 700nm] : BDHR_VIS and BBHR_VIS
- whole spectrum [300 – 4000nm] : BDHR and BBHR

The general narrow to broadband relationship is according to Eq. 13. The respective errors are estimated following the Eq. 14:

Eq. 13 $$Broadband = \alpha_0 + \alpha_4 * 490nm + \alpha_5 * 565nm + \alpha_6 * 670nm + \alpha_7 * 765nm + \alpha_8 * 865nm$$

Eq. 14 $$ErrBroadband = \alpha_4 * Err490nm + \alpha_5 * Err565nm + \alpha_6 * Err670nm + \alpha_7 * Err765nm + \alpha_8 * Err865nm$$

The conversion coefficients are specified by Météo-France/CNRM and presented in the following table.

Broad Band	α_0	α_4	α_5	α_6	α_7	α_8
[400 - 700nm]	- 0.0060	0.2599	0.2334	0.4792	0	0
[300 - 4000nm]	0.0383	0.0394	0.0243	0.3078	0.2501	0.1510

Table 1 : Narrow to broadband conversion coefficients

3.2.3. The Normalized Difference Vegetation Index

The Normalized Difference Vegetation Index (NDVI), corrected for the directional effects, is derived from DHR_{670nm} and DHR_{865nm} (Eq. 15) , and its error is calculated by Eq. 16.

Eq. 15

$$NDVI = \frac{\mathrm{DHR}_{865} - \mathrm{DHR}_{670}}{\mathrm{DHR}_{865} + \mathrm{DHR}_{670}}$$

Eq. 16

$$ErrNDVI = 2 * \mathrm{DHR}_{865} * \mathrm{NDVI} * \frac{\mathrm{ErrDHR}_{865} + \mathrm{ErrDHR}_{670}}{\left(\mathrm{DHR}_{865} + \mathrm{DHR}_{670}\right)^2}$$

4. Conclusion

The algorithms presented in this document have been initially developed for POLDER-1 and POLDER-2 measurements, and improved to be applied to POLDER-3 data. The POLDER-3/PARASOL BRDF and albedo products have been validated by Météo-France/CNRM. The products and the validation report are available on the POSTEL website at the address: http://postel.mediasfrance.org/en/DOWNLOAD/.

5. References

Bréon, F.M. and S. Bouffiès, Land surface pressure estimate from measurements in the oxygen A absorption band, *Journal of Applied Meteorology, 35, 69-77*, 1996

Bréon, F.M., and S. Colzy, Cloud detection from the spaceborne POLDER instrument and validation against surface synoptic observations, *Journal of Applied Meteorology, 28, 777-785*,1999.

Bréon, F.M., F. Maignan, M. Leroy and I. Grant, Analysis of hot spot directional signatures measured from space. *Journal of Geophysical Research, 107 (16), 4,282-4,296,* 2002.

Dubovik, O., B.N. Holben, T.F. Eck, A.Smirnov, Y.J. Kaufman, M.D. King, D. Tanré and I. Slutsker, Variability of absorption and optical properties of key aerosol types observed in worldwide locations, *Journal of the Atmospheric Sciences, 59: 590-608,* 2002.

Maignan, F., F.M. Bréon and R. Lacaze, Bi-directional reflectance of Earth targets : evaluation of analytical models using a large set of spaceborne measurements with emphasis on the Hot Spot, *Remote Sensing of Environment, 90, 210-220,* 2004.

Roujean, J. L., M. Leroy and P. Y. Deschamps, A bi-directional reflectance model of the Earth' s surface for the correction of remote sensing data, *Journal of Geophysical Research, 97, D18, 20,455-20,468,* 1992.

Vermote, E.F., D. Tanré, J.L. Deuzé, M. Herman, J.J. Morcrette, Second Simulation of the Satellite Signal in the Solar Spectrum, 6S : an overview. *IEEE Transactions on Geoscience And Remote Sensing, 35 (3): 675-686*, 1997.

Walthall, C. L., J. M. Norman, J. M. Welles, G. Campbell and B. L. Blad, Simple equation to approximate the bi-directional reflectance from vegetative canopies and bare soil surfaces, *Applied Optics, 24, 383-387*, 1985.

6. Acknowledgement and contacts

Development of the "Land Surface" Level 2 algorithms results from a collaboration between the Laboratoire des Sciences du Climat et de l'Environnement (LSCE) et le Laboratoire d'Optique Atmosphérique (LOA).

Development of the “Land Surface” Level 3 algorithms results from a collaboration between the LSCE and the Centre National de Recherches Météorologiques (CNRM).

These developments have been supported by the Centre National d’Etudes Spatiales (Cnes).

The production of Land Surface Level 2 and Level 3 products is carried out by Postel, the pole of thematic competences on land surfaces, located at Medias-France. The POLDER-3/PARASOL are available for downloading through the Postel web site at the address: http://postel.mediasfrance.org.

This document is based upon technical documents provided by Medias-France. It is available, like all documents relating to POLDER-3/PARASOL products, on the Postel web site.

For any question concerning the algorithms, the products, or the validation process, please contact: roselyne.lacaze@cesbio.cnes.fr